International Journal of Nanomedicine

Dovepress
open access to scientific and medical research

Open Access Full Text Article

ORIGINAL RESEARCH

Ultrasonographic Contrast and Therapeutic Effects of Hydrogen Peroxide-Responsive Nanoparticles in a Rat Model with Sciatic Neuritis

Da-Sol Kim[1,2,*], Nam-Gyu Jo[3,*], Dong-Won Lee[4,5], Myoung-Hwan Ko[1,2], Jeong-Hwan Seo[1,2], Gi-Wook Kim[1,2,4]

[1]Department of Physical Medicine & Rehabilitation, Jeonbuk National University Medical School, Jeonju, Republic of Korea; [2]Research Institute of Clinical Medicine of Jeonbuk National University-Biomedical Research Institute of Jeonbuk National University Hospital, Jeonju, Republic of Korea; [3]Department of Physical Medicine and Rehabilitation, Hansol Convalescence Rehabilitation Hospital, Jeonju, Republic of Korea; [4]Department of Bionanotechnology and Bioconvergence Engineering, Jeonbuk National University, Jeonju, Republic of Korea; [5]Department of Polymer Nano Science and Technology, Jeonbuk National University, Jeonju, Republic of Korea

*These authors contributed equally to this work

Correspondence: Gi-Wook Kim, Department of Physical Medicine & Rehabilitation, Jeonbuk National University Medical School, Geonjiro 20, Deokjin-gu, Jeonju, Jeonbuk, 54907, Republic of Korea, Tel +82-63-259-3144, Fax +82-10-254-4145, Email k26@jbnu.ac.kr

Purpose: Peripheral nerve damage lacks an appropriate diagnosis consistent with the patient's symptoms, despite expensive magnetic resonance imaging or electrodiagnostic assessments, which cause discomfort. Ultrasonography is valuable for diagnosing and treating nerve lesions; however, it is unsuitable for detecting small lesions. Poly(vanillin-oxalate) (PVO) nanoparticles are prepared from vanillin, a phytochemical with antioxidant and anti-inflammatory properties. Previously, PVO nanoparticles were cleaved by H_2O_2 to release vanillin, exert therapeutic efficacy, and generate CO_2 to increase ultrasound contrast. However, the role of PVO nanoparticles in peripheral nerve lesion models is still unknown. Herein, we aimed to determine whether PVO nanoparticles can function as contrast and therapeutic agents for nerve lesions.

Methods: To induce sciatic neuritis, rats were administered a perineural injection of carrageenan using a nerve stimulator under ultrasonographic guidance, and PVO nanoparticles were injected perineurally to evaluate ultrasonographic contrast and therapeutic effects. Reverse transcription-quantitative PCR was performed to detect mRNA levels of pro-inflammatory cytokines, ie, tumor necrosis factor-α, interleukin-6, and cyclooxygenase-2.

Results: In the rat model of sciatic neuritis, PVO nanoparticles generated CO_2 bubbles to increase ultrasonographic contrast, and a single perineural injection of PVO nanoparticles suppressed the expression of tumor necrosis factor-α, interleukin-6, and cyclooxygenase-2, reduced the expression of F4/80, and increased the expression of GAP43.

Conclusion: The results of the current study suggest that PVO nanoparticles could be developed as ultrasonographic contrast agents and therapeutic agents for nerve lesions.

Keywords: neuroinflammation, ultrasonography, contrast media, polymer nanoparticles, hydrogen peroxide

Introduction

The nervous system is specialized and highly organized. Peripheral nerves extend from the central nervous system, the most important organ, enabling the entire body to communicate and coordinate in response to various environmental changes.[1] However, peripheral nerves are frequently damaged due to compression, traction, laceration, infection, or ischemia.[2] Peripheral nerve injury is frequently encountered in the clinical field of the musculoskeletal system. Consequently, peripheral nerve damage is frequently associated with paralysis, sensory loss, or neuropathic pain, which leads to an inconvenient life.[3]

In neuropathy caused by mild insults, such as compression, the intraneural venous circulation is first disturbed; if it persists, edema occurs due to a disorder of the blood-nerve interface, eventually leading to intraneural and extraneural fibrosis.[4,5] Prolonged compromise may induce downstream effects, such as demyelination and, ultimately, axon degeneration.[6]

Received: 1 November 2023
Accepted: 19 February 2024
Published: 27 March 2024

Neuroinflammation progresses with neurostructural abnormalities, and immune cells are activated by damaged neurons. The subsequent activation of immune mediators (eg, cytokines, chemokines, and lipid mediators) decreases the neural threshold and may lead to peripheral sensitization and increased sensitivity to afferent nerve stimuli.[7] Extensive research on neuroinflammation concerning nerve degeneration, regeneration, and neuropathic pain has been conducted, which are all well-known key factors in the pathophysiology and treatment strategies of neuropathies.[8,9]

Ultrasonography (US) is an irreplaceable modality for diagnosing peripheral nerve pathologies and guiding perineural interventions. Moreover, US is easily accessible, affordable, minimizes patient discomfort, and enables dynamic real-time examinations when compared with magnetic resonance imaging (MRI) or electrodiagnostic studies.[10] US findings in neuropathic conditions include hypoechoic edematous swelling of nerve fascicles, increased cross-sectional area, and compression ratio.[11] However, detecting the precise location of focal small nerve lesions and inflammation with microstructural and adjuvant soft tissue abnormalities remains challenging, despite confirming abnormalities in nerve conduction studies. Additionally, inaccurate localization of nerve lesions during US-guided interventions may decrease therapeutic outcomes and increase the risk of secondary complications.[12,13] The use of contrast agents can increase the diagnostic value of US. However, only gas-filled microbubble agents for internal organs such as the liver and kidneys have been established, and contrast agents for nerves remain poorly developed.[14]

Treatment options for peripheral neuropathy or traumatic nerve injury range from conservative to surgical intervention. Conservative treatment includes education, splinting, physical therapy, nerve gliding exercises, pharmacological interventions, and corticosteroid injection therapy.[15,16] Corticosteroids suppress pro-inflammatory cytokines and exert therapeutic effects by suppressing inflammation and edema. Typically, corticosteroids are recommended as effective drugs, although local or systemic adverse events, such as necrosis or atrophy of adjacent musculoskeletal tissues or loss of bone density, can occur. Furthermore, contraindications such as drug allergies, infections, and hyperglycemia are commonly encountered; however, satisfactory alternatives are insufficient.[17,18] Despite the recent expansion of knowledge of neuronal recovery mechanisms, satisfactory motor and sensory function recovery is not assured, even with current clinical treatment.[19]

Ultrasonographic contrast effects of poly(vanillin-oxalate) (PVO) nanoparticles have been previously reported, along with their anti-inflammatory and anti-apoptotic activities in a rat model with muscle injury.[20] Vanillin, a therapeutic agent, is extracted from the seed pods of *Vanilla planifolia* and is an antioxidant substance that scavenges superoxide anions and hydroxyl radicals and inhibits protein oxidation and lipid peroxidation. In addition, vanillin is known to exert anti-inflammatory activity by suppressing the expression of several pro-inflammatory cytokines, along with antimicrobial and anticancer effects.[21,22] The synthesis of PVO nanoparticles from vanillin may broaden its therapeutic applications. PVO nanoparticles have acid-cleavable acetal and peroxalate ester linkages that are degraded by H_2O_2, which is well-known to be elevated in damaged or inflamed tissues. Vanillin is released during degradation, and simultaneously, CO_2 bubbles are generated, which enable the function of echogenic agents to increase the US contrast. Previous studies have demonstrated the potential of H_2O_2-responsive PVO nanoparticles as therapeutic and US contrast agents for muscle injury; however, their role in peripheral nerves, which are smaller and have complex tissues, remains unexplored.[23,24]

In the present study, we assessed the diagnostic and therapeutic potential of H_2O_2-triggered echogenic anti-inflammatory PVO nanoparticles in a rat model of carrageenan-induced sciatic neuritis. The sciatic nerve is the most widely utilized model for investigating the pathophysiology of peripheral nerve damage owing to its large size and relatively easy access.[25] Moreover, we explored whether PVO nanoparticles could exert beneficial therapeutic effects and increase US contrast by generating CO_2 in the rat model of sciatic neuritis to establish the value of PVO nanoparticles for the diagnosis and treatment of nerve lesions.

Methods

Preparation of PVO Nanoparticles

PVO was synthesized by polymerization of an acid-cleavable vanillin derivative and oxalyl chloride, as previously reported.[20] Briefly, the acid-cleavable vanillin derivative was added to a flask containing 25 mL dry dichloromethane and pyridine (9.8 mmol). The flask was placed in an ice bath, followed by the addition of oxalyl chloride (3.941 mmol); the

mixture was maintained at room temperature for 6 h. PVO was obtained by extraction with dichloromethane/water and precipitation in cold hexane. The chemical structure of the PVO was analyzed using nuclear magnetic resonance spectroscopy (JNM-ECZ500R, JEOL, Akishima, Japan) and Fourier transform infrared (FT-IR) spectrometer (Spectrum 3, Perkin Elmer, Shelton, USA) after purification. PVO nanoparticles were prepared using a previously reported single-emulsion method.[20] PVO nanoparticles suspended in water or lysates from neurite tissue 24 h after induction were characterized using a scanning electron microscope (SUPRA40VP, Carl Zeiss, Jena, Germany) and nanoparticle size analyzer (Brookhaven Instruments Corporation, Holtsville, NY, USA) using dynamic light scattering.

Rat Model of Carrageenan-Induced Sciatic Neuritis

The sciatic nerve is frequently used in preclinical nerve injury studies owing to its large size and easy accessibility.[26] Sprague Dawley rats (8-week-old males; Orient Bio, Seongnam, Korea) were anesthetized by intraperitoneal administration of a mixture of ketamine and xylazine (8:1). To maintain anesthesia, isoflurane (Ifran Solution, Hana Pharm, Seoul, Korea) was administered in 100% oxygen using a vaporizer. Subsequently, with the rat in a prone position with a slightly stretched leg, the sciatic nerve was confirmed using US and a nerve stimulator, and 200 μL of 10 mg/mL carrageenan was administered perineurally (Figure 1).[27]

For functional evaluation of the established model, footprint tests were performed by walking rats on white paper to track ink-stained hind paws. To measure H_2O_2 levels at the site of sciatic neuritis, nerve tissues were extracted 3, 6, and 24 h after inducing sciatic neuritis. The tissues were lysed in phosphate-buffered saline at a concentration of 10 mg/mL using a homogenizer and centrifuged at 8000×g for 10 min to obtain supernatants. H_2O_2 levels in the supernatant were determined using an Amplex Red Assay Kit (Invitrogen, Carlsbad, CA, USA) and a microplate reader (Biotek Instruments, Winooski, VT, USA). The fluorescence intensities of normal nerves (sham) and neuritic tissues were compared.

Experimental Procedure

Sprague–Dawley rats (8-week-old males, Orient Bio, Seongnam, Korea) were randomly allocated to three groups: a sham group (n = 6) as the normal control, an untreated group (n = 6), which underwent carrageenan-induced sciatic neuritis, and a PVO group (n = 6) for enzyme-linked immunosorbent assay (ELISA) and reverse transcription-quantitative polymerase chain reaction (RT-qPCR). All perineural injections were administered under ultrasonographic guidance using a nerve

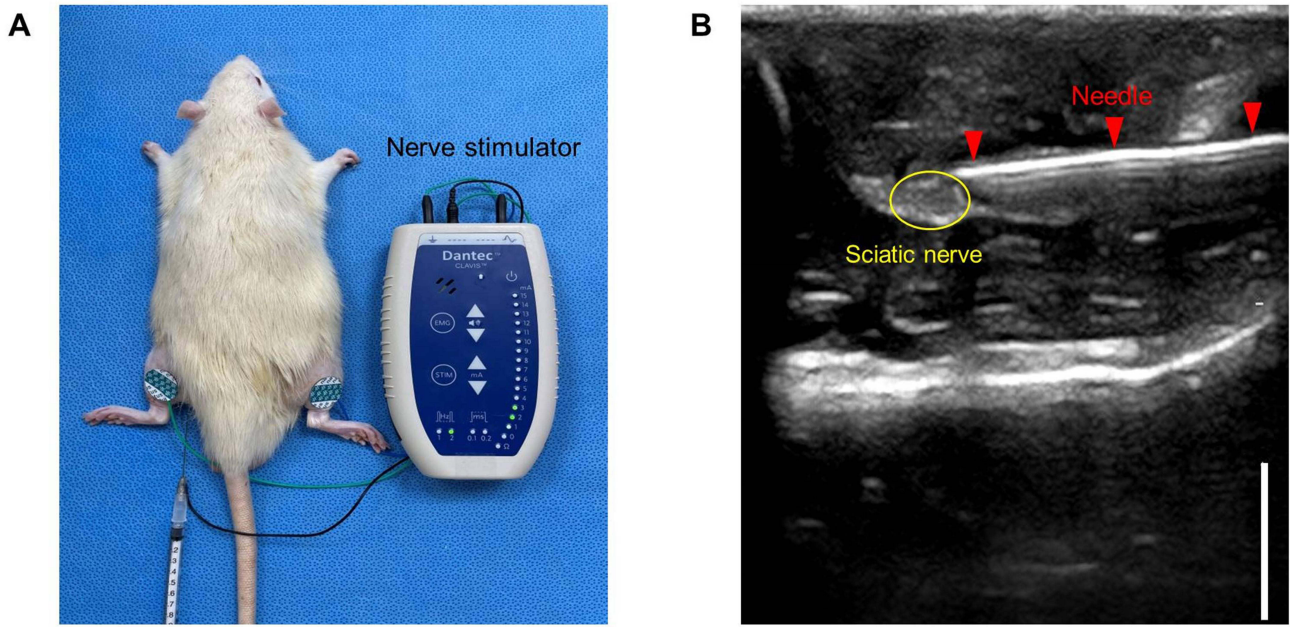

Figure 1 Rat model of sciatic neuritis established using a nerve stimulator and ultrasound-guided carrageenan injection. (**A**) Rat modeling using nerve stimulator. (**B**) Imaging of ultrasound-guided injection. The scale bar is 5 mm.

stimulator. The sciatic nerve tissue was extracted 48 h after neuritis induction in the untreated group. In the PVO group, PVO nanoparticles were injected 24 h after neuritis induction, and sciatic nerves were extracted 24 h later.

Enhanced Ultrasonographic Imaging of Sciatic Neuritis Using PVO Nanoparticle Contrast

For US imaging, PVO nanoparticles (200 μL of 10 mg/mL in saline) were perineurally injected around the lesion site using a nerve stimulator under ultrasound guidance 24 h after sciatic neuritis induction. Additionally, US images were obtained by injecting SonoVue® (Bracco, Milan, Italy) and normal saline around the sciatic nerve or neurite. A US instrument (Zone Ultra, Zonare Medical Systems, San Francisco, CA, USA) with a broadband hockey-stick linear transducer (5–14 MHz) was employed. A physician proficient in musculoskeletal US acquired US images in long- and short-axis views. All animal experimental procedures were approved by the Institutional Animal Care and Use Committee (IACUC) of Jeonbuk National University Hospital (CUH-IACUC-2021-34-1) and were performed following the regulations.

ELISA

PVO nanoparticles (200 μL of 10 mg/mL) were perineurally injected around the lesion site after 24 h of sciatic neuritis induction. The sciatic nerve was excised 24 h post-injection of PVO nanoparticles. After homogenization and centrifugation, the medium and standards were pipetted and analyzed using ELISA (Proteintech Group, Chicago, IL, USA) for tumor necrosis factor (TNF)-α and interleukin (IL)-6. After combining primary and secondary antibodies, the color of the bound substance was changed by the application of substrate and stop solutions. The color intensity reflects the degree of cytokine binding. Cytokine levels were calculated in picograms (cytokines)/mL(medium) using curves plotted from standard solutions and recorded using a commercial microplate reader system (TECAN, Spectrafluor Plus, Tecan Group Ltd., Männedorf, Switzerland).

RT-qPCR

Twenty-four hours after injecting PVO nanoparticles (200 μL of 10 mg/mL), the sciatic nerves were excised and homogenized with TRIzol reagent (Invitrogen, Carlsbad, CA). Total RNA (1 μg) was treated with RNase-free DNase, and first-strand cDNA was prepared using a random hexamer primer provided in the First-Strand cDNA Synthesis kit (TaKaRa Bio, Otsu, Japan, ##RR037A) according to the guidelines of the manufacturer. cDNA was amplified using PCR with specific primers and thermal cycling conditions for TNF- α, IL-6, cyclooxygenase (COX)-2, and GAPDH. Table 1 lists all primers (Bioneer, Daejeon, Korea) used in the present study. RT-qPCR was performed using a real-time PCR system (Applied Biosystems QuantStudio 6 Flex Real-Time PCR System; Marsiling, Singapore).

Table 1 Sequences and Accession Numbers for Primers (Forward, F; Reverse, R) Used in Reverse Transcription-Quantitative PCR

Target Genes	Primer Sequence	Accession No.
TNF-α	F: 5′-CAG GAG AAA GTC AGC CTC CTC −3′	NM_012675.3
	R: 5′-CCA GGT ACA TGG GCT CAT ACC −3′	
IL-6	F: 5′-AAG AGA CTT CCA GCC AGT TGC −3′	NM_012589.2
	R: 5′-TGG TCT GTT GTG GGT GGT ATC −3′	
COX-2	F: 5′-CAG CCA TAC TAT GCC TCG GA −3′	NM_017232
	R: 5′-GGA TGT CTT GCT CGT CGT TC −3′	
GAPDH	F: 5′- CAT GGC CTT CCG TGT TC −3′	NM_017008

Abbreviations: COX-2, cyclooxygenase-2; ELISA, enzyme-linked immunosorbent assay; IL-6, interleukin-6; PVO, Poly(vanillin-oxalate); MRI, magnetic resonance imaging; PBS, phosphate-buffered saline; S.D., standard deviation; TNF-α, tumor necrosis factor-α; US, ultrasonography; NMR, nuclear magnetic resonance; FT-IR, Fourier transform infrared.

Immunofluorescence Staining

Slides used for immunofluorescence staining were fixed with formaldehyde (4%) solution and embedded in paraffin. Tissue sections were co-incubated with primary antibodies against growth-associated protein 43 (GAP43), a nerve regeneration marker, and F4/80, a macrophage marker.

Statistical Analysis

Statistical analyses were performed using IBM SPSS version 23.0 (IBM Corp., Armonk, NY, USA). Quantification by ELISA and RT-qPCR was conducted using one-way analysis of variance (ANOVA) for the three groups (Sham, Untreated, and PVO groups). The Bonferroni method or Dunnett's T3 method were performed as post-hoc tests, depending on whether equal variances were satisfied. p values < 0.05 were considered statistically significant (n = 6).

Results

Characterization of PVO Nanoparticles

PVO was synthesized by reacting an acid-cleavable vanillin derivative with oxalyl chloride (Figure 2A). PVO was designed to undergo H_2O_2-induced degradation to produce vanillin and CO_2. ^{1}H NMR spectroscopy indicated that the methylene next to peroxalate ester bonds appeared at ~4.6 ppm and the acetal proton was observed at ~5.5 ppm

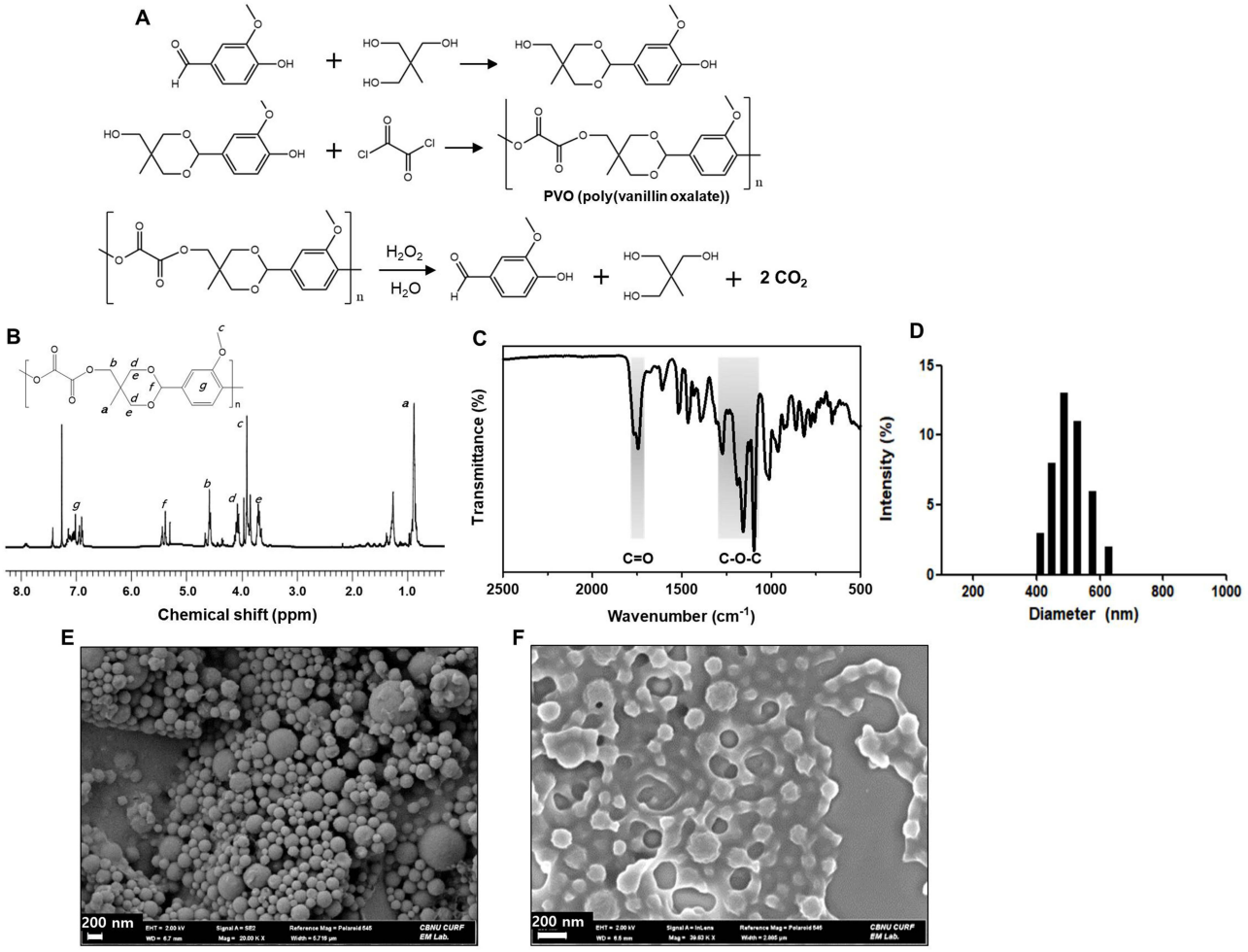

Figure 2 Characterization of PVO nanoparticles. (**A**) Synthetic route and chemical structure of PVO and H_2O_2-triggered degradation for CO_2 generation. (**B**) ^{1}H NMR spectrum of PVO in $CDCl_3$. (**C**) Infrared spectrum of PVO nanoparticles. (**D**) Size distribution of PVO nanoparticles dispersed in PBS. (**E**) Representative SEM image of PVO nanoparticles. (**F**) SEM images showing the degradation of PVO nanoparticles in supernatants from inflamed nerve tissue.
Abbreviations: PVO, Poly(vanillin-oxalate); NMR, nuclear magnetic resonance; SEM, scanning electron microscope.

(Figure 2B). FT-IR analysis revealed that the C=O stretching vibration in peroxalate was observed at 1700 cm^{-1} and C-O-C stretching vibration was at 1150 cm^{-1} (Figure 2C). The PVO nanoparticles were monodisperse spheres with a mean hydrodynamic diameter of approximately 500 nm (Figure 2D and E). PVO nanoparticles showed surface degradation during incubation with supernatants derived from the inflamed nerve tissues (Figure 2F).

Carrageenan-Induced Sciatic Neuritis Model

After model induction, footprint tests were performed to evaluate the adequacy of the model. Weak footprinting due to paralysis appeared on the left side, indicating the induction of neuritis (Figure 3A). In addition, the Amplex Red assay was performed to confirm elevated H_2O_2 levels, revealing an increase over 3, 6, and 24 h after carrageenan injection (Figure 3B).

Ultrasonographic Imaging of Sciatic Neuritis Enhanced by PVO Nanoparticle Contrast

SonoVue produced nonspecific contrast enhancement along the diffusion path following the perineural injection of SonoVue and PVO nanoparticles at the normal sciatic nerve, despite the absence of lesions owing to the inherent characteristics of its microbubbles. Conversely, PVO nanoparticles did not show enhancement in non-lesional areas (Figure 4A).

Next, the H_2O_2-triggered echogenicity of PVO nanoparticles was evaluated in a rat model of sciatic neuritis. A slightly hypoechoic swollen fascicle on the sciatic nerve was suspected on non-contrast US images; nevertheless, it was not prominent. SonoVue generated a clinically meaningless contrast pattern similar to that of normal nerves and did not exhibit lesion-specific properties. As a control, no contrast change was observed after normal saline injection; however, the PVO nanoparticles showed noticeable lesion-specific contrast enhancement only in the inflamed area (Figure 4B and Supplementary Video S1). On follow-up US after the PVO injection, the increased contrast gradually weakened and disappeared at 3 h (Figure 4C).

Therapeutic Effects of PVO Nanoparticles on Sciatic Neuritis

To assess the anti-inflammatory activities of PVO nanoparticles in sciatic neuritis, protein and mRNA expression levels of pro-inflammatory cytokines were investigated using ELISA and RT-qPCR, respectively (n = 6). ELISA results are expressed as cytokine levels measured in the sham, untreated, and PVO groups (pg/mL ± standard deviation). TNF-α levels were significantly increased in the untreated group when compared with those of the sham group ($p < 0.001$); levels were significantly decreased in the PVO group when compared with those in the untreated group ($p < 0.001$). The untreated group exhibited significantly higher IL-6 levels than the sham group ($p < 0.001$), while the PVO group had significantly lower levels than the untreated group ($p < 0.001$). PVO significantly suppressed TNF-α and IL-6, although

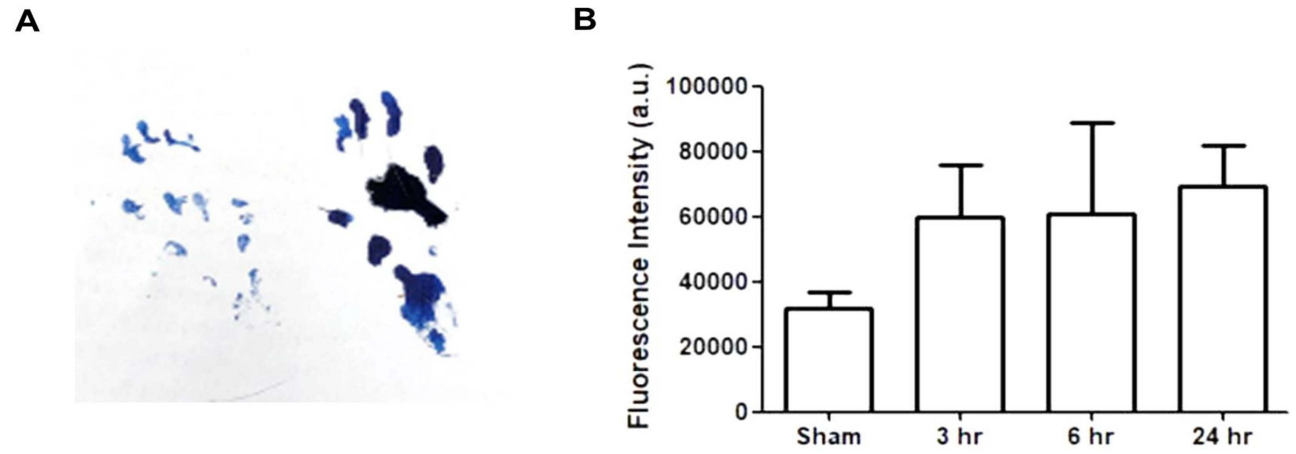

Figure 3 Evaluations of the neuritis model. (**A**) Footprint results of the left sciatic nerve injury model. (**B**) Amplex Red assay results for the normal nerve (sham), and 3, 6, and 24 h after rat modeling.

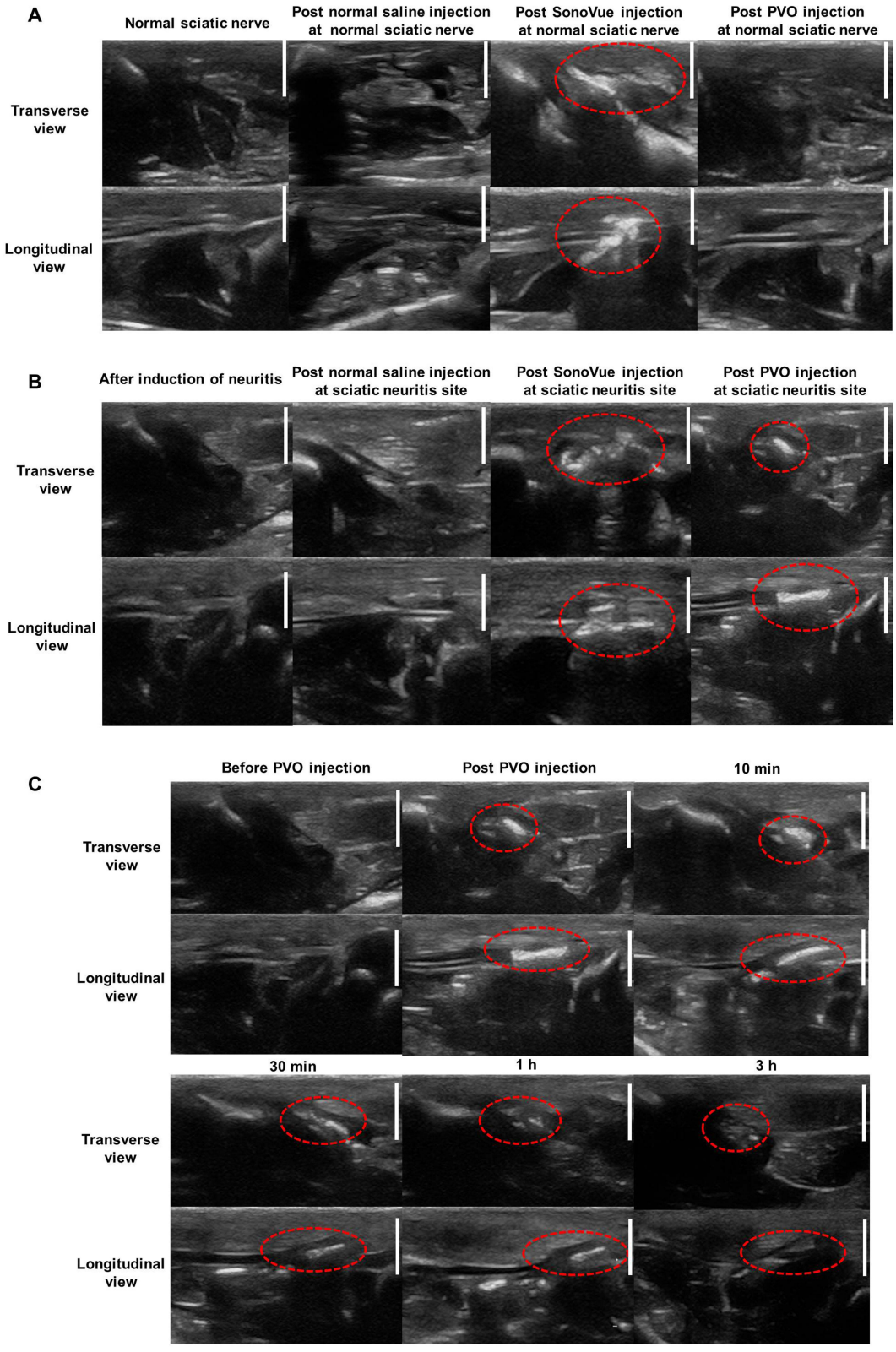

Figure 4 Ultrasonographic imaging of sciatic nerve in transverse and longitudinal view. (**A**) Ultrasonographic images after perineural injection of SonoVue and PVO nanoparticles at the normal sciatic nerve. The normal nerve exhibits enhancement beyond the area around the nerve where SonoVue has spread. (**B**) Ultrasonographic images using normal saline, SonoVue, and PVO nanoparticles targeting neuritis sites. SonoVue generates a clinically meaningless contrast pattern, while PVO nanoparticles exhibit a lesion-specific contrast effect. (**C**) Ultrasonographic images enhanced by PVO nanoparticles and follow-up images. It gradually fades and disappears at 3 h. The scale bar is 5 mm.

Abbreviation: PVO, Poly(vanillin-oxalate).

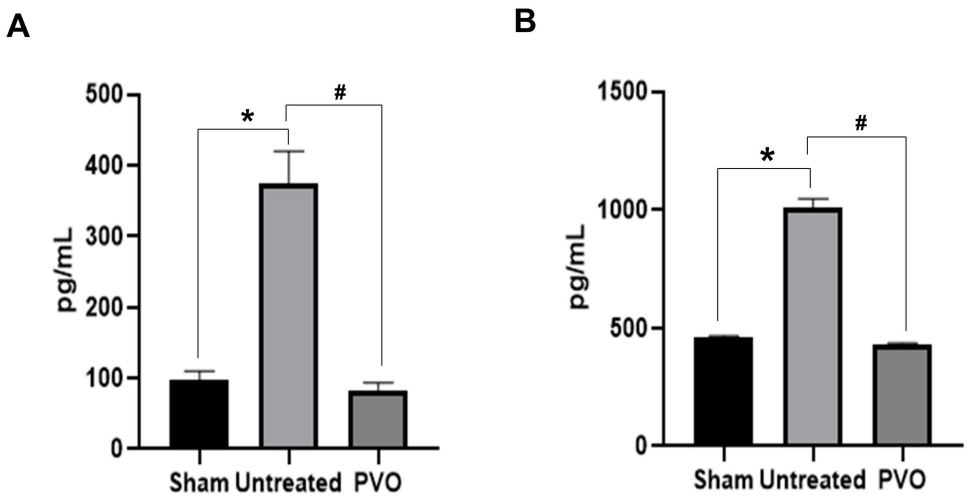

Figure 5 Anti-inflammatory effects of PVO nanoparticles in a rat model of sciatic neuritis using ELISA. Expression of (**A**) TNF-α and (**B**) IL-6. After PVO injection, the pro-inflammatory cytokine (TNF-α and IL-6) levels are reduced when compared with those of the untreated group. Values are mean ± S.D. (n = 6). *$p < 0.001$ in Sham vs PVO; #$p < 0.001$ in untreated vs PVO.
Abbreviations: ELISA, enzyme-linked immunosorbent assay; IL-6, interleukin-6; PVO, Poly(vanillin-oxalate); S.D., standard deviation; TNF-α, tumor necrosis factor-α.

no statistically significant difference was observed when compared with these levels in the sham ($p = 0.226$ and $p = 0.304$, respectively) (Figure 5).

In addition, the mRNA expressions of pro-inflammatory cytokines were evaluated using RT-qPCR. Carrageenan-induced neuroinflammation increased examined mRNA levels significantly ($p < 0.001$), whereas perineural injection of PVO significantly decreased TNF-α ($p = 0.013$), IL-6 ($p < 0.001$), and COX-2 ($p = 0.003$) levels (Figure 6).

Immunofluorescence Staining

The inflammatory cell infiltration into the lesion was examined by staining with F4/80 antibody, a macrophage marker. PVO nanoparticles suppressed carrageenan-induced nerve damage and macrophage infiltration. GAP43 is an intracellular growth-associated protein and a proven marker of neuronal development and regeneration.[28]

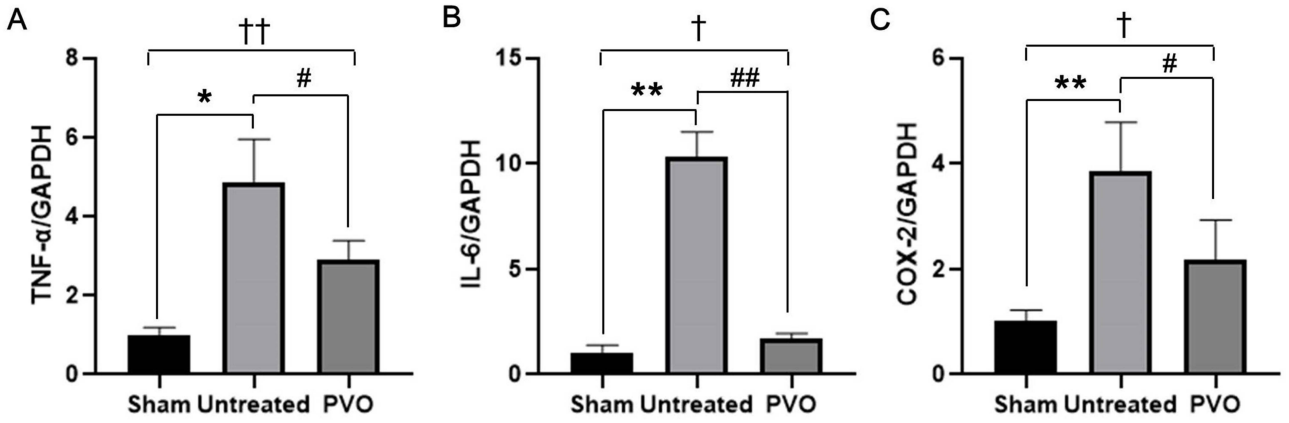

Figure 6 Anti-inflammatory effects of PVO nanoparticles in a rat model of sciatic neuritis using RT-qPCR. mRNA levels of pro-inflammatory cytokines ((**A**) TNF-α, (**B**) IL-6, (**C**) COX-2) are significantly reduced when compared with those of the untreated group after PVO injection. Values are mean ± S.D. (n = 6). *$p < 0.05$, **$p < 0.001$ in Sham vs PVO; #$p < 0.05$, ##$p < 0.001$ in Untreated vs PVO; †$p < 0.05$, ††$p < 0.001$ in Sham vs PVO.
Abbreviations: COX-2, cyclooxygenase-2; IL-6, interleukin-6; PVO, Poly(vanillin-oxalate); S.D., standard deviation; TNF-α, tumor necrosis factor-α.

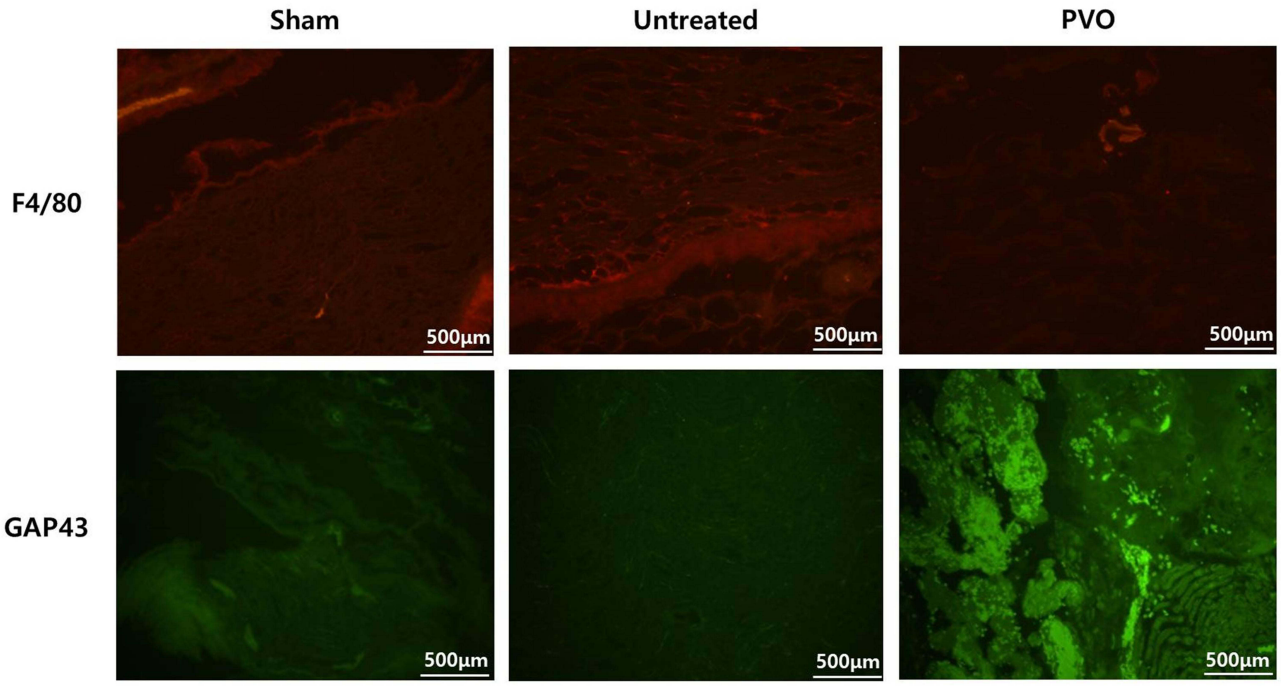

Figure 7 Immunofluorescence staining. The PVO group exhibits reduced F4/80 (macrophage marker) expression when compared with the sham and untreated groups. The PVO group shows higher GAP43 staining (nerve regeneration marker) at the site of neuritis than the sham and untreated groups.

GAP43 expression was decreased in damaged tissues; nevertheless, PVO nanoparticles increased GAP43 expression (Figure 7).

Discussion

Neuroinflammation is a crucial pathogenesis in any type of peripheral neuropathy, whether entrapment neuropathy or traumatic nerve injury, as pro-inflammatory cytokines are key modulators facilitating the interaction between immune cells, neurons, and Schwann cells during the processes of degeneration, regeneration, and pain.[29] Immediately after peripheral nerve damage, TNF-α expression increases at the site of the lesion, leading to massive recruitment of macrophages mediated by upregulation of metalloproteinase, adhesion molecules (intercellular adhesion molecule, ICAM; vascular cell adhesion molecule, VCAM), and other cytokines (IL-1α, IL-1β, IL-6, and IL-8) from activated immune cells.[30,31] Matrix metallopeptidase-9 (MMP-9), produced by Schwann cells and endoneurial macrophages, participates in blood-nerve barrier degradation and myelin phagocytosis.[32] Neuroinflammation has been implicated as a key factor in the development of neuropathic pain, defined as pain originating from damage or dysfunction of the somatosensory system.[33] Neuropathic pain has an enormously complex pathophysiology involving deleterious structural and physiological changes from the injury site of the peripheral nerve to the descending modulatory pathways in the brain and spinal cord.[34] The basis for the development of neuropathic pain is aberrant neurophysiological discharge mediated by pro-inflammatory cytokines.[35] During neuroinflammation, the activation of immune cells and upregulation of cytokines and chemical mediators, such as histamine, bradykinin, acids, and serotonin, bring the nerve membrane potential closer to the depolarization threshold. The receptors at the nociceptive terminals are more easily stimulated, ion channels are upregulated, and nociceptors are more sensitized to stimulation at the same intensity (peripheral sensitization). If pain is not relieved and inflammation continues, the excitation of spinal neurons, which are ultimately linked to the reverse transport of cytokines and their receptors to the spinal cord nerve, leads to central sensitization.[33,36]

MRI, US, and electrodiagnostic studies are commonly used as diagnostic tools for neuropathy.[37] Electrodiagnostic testing is particularly helpful in diagnosing distal neuropathies (eg, carpal tunnel syndrome); however, they can be uncomfortable, and if nerve conduction is completely lost, accurately localizing the lesion can be difficult. Although

important for early diagnosis, the diagnostic power is maximized 2 weeks after Wallerian degeneration is completed.[38] MRI is particularly useful for the diagnosis of proximal neuropathies (eg, sciatica). However, false negative results or cases that do not match other clinical conditions are often encountered.[39] US has the advantage of being cost-effective, convenient to access, and easy to compare with the contralateral side. However, US has a relatively poor contrast resolution, is less sensitive to changes in tissue fluid, making it unsuitable for the diagnosis of small focal lesions, and allows limited visualization of deep (> 5 cm) nerves.[40,41] Crucially, considerable operator dependence on image acquisition and interpretation complicates the diagnosis and treatment processes.[41]

Contrast-enhanced ultrasound is the key to overcoming these limitations despite technological advances in US, such as high-resolution and electronic broadband transducers. However, ultrasonographic contrast agents for the musculoskeletal system, including nerves, may require additional data for clinical application.[42] The currently used ultrasonographic contrast agents include microbubbles composed of gas-filled shells. Microbubbles interact with ultrasonic waves to resonate and oscillate, creating a specific harmonic signal that can be distinguished from the surrounding tissue.[43] Ultrasonographic contrast agents have gradually improved to increase shell stability using gases with low solubility. Currently, commercial contrast agents include SonoVue (sulfur hexafluoride microbubbles) and Definity (perflutren lipid microspheres). However, these contrast agents mainly target the heart or internal organs of the abdomen.[44] SonoVue (Bracco, Milan, Italy) is the most commonly used contrast agent for internal organs and contains microbubbles with a mean diameter of 1.5–2.5 mm, comprising a sulfur hexafluoride core and a stabilizing phospholipid shell, targeting the musculoskeletal system. However, the contrast peak time was short (approximately a few seconds), accompanied by poor localization.[45] SonoVue was originally developed as an intravascular contrast agent. Owing to its intrinsic properties, SonoVue functions as a contrast agent by itself and is a nonspecific contrast agent for musculoskeletal pathology.[46]

A carrageenan-induced neuritis model was used to determine lesion (nerve)-specific contrast effects. Other sciatic nerve injury models include transection, compression, and ligation;[25] however, these models often introduce adjacent muscular damage and inflammation, deemed unsuitable for the current study. If the current study used previous methods, ie, nerve injury models involving transection, compression, and ligation, diffuse enhancements may have been observed across the muscle layer and nerve with US. Therefore, we used a focal neuritis model with a perineural injection of carrageenan, which is commonly used to examine inflammation-induced damage to nerves, tendons, and muscles.[47] The accuracy of the injection was improved by using nerve stimulation under ultrasonographic guidance, and neuritis-induced paralysis was confirmed using footprinting analysis on a functional scale. In addition, the Amplex Red assay was used to assess increased H_2O_2 levels after neuritis induction, which reflected carrageenan-induced neuroinflammation.

Herein, we aimed to determine whether perineural injection of PVO nanoparticles increases echogenicity in inflamed areas using US. During this experiment, PVO nanoparticles injected at one point diffused to a certain extent along the course of the sciatic nerve, causing an increase in contrast. In clinical practice, accurate localization using US is often challenging despite symptoms or electrodiagnostic examination results suggestive of neuropathy.[48] Injecting PVO nanoparticles may facilitate the identification of suspicious nerve lesions or lesions that do not demonstrate specific findings in electrodiagnostic or imaging studies. CO_2 bubbles generated following H_2O_2-triggered oxidation of the peroxalate esters of PVO are echogenic.[49] Using a muscle injury model, we previously reported a marked increase in the echo signal, which increased to 2 h and disappeared at 3 h after PVO injection.[23] Immediate and sufficient contrast enhancement was observed in the neuritis model. In addition, previous results on the difference in duration between the muscle tissue and the agarose gel phantom suggested that the duration of the contrast effect would be prolonged in a more closed system or at high H_2O_2 levels.[23] Herein, the value of PVO nanoparticles as lesion-specific contrast agents was demonstrated in comparison with that of SonoVue, which is inevitably a non-lesion-specific contrast agent owing to the inherent properties of microbubbles, with normal saline used as a control. Pathological stimulus-induced echogenicity of sufficient duration would greatly assist physicians in diagnosing small or mild neuronal damage.

Controlling neuroinflammation is an important factor in treating neuropathy or neuropathic pain. A preclinical study using TNF-α deficient mice revealed reduced macrophage recruitment and axon and myelin degradation after sciatic nerve injury.[50] In another model of chronic nerve constriction injury, decreased mRNA expression of IL-1β and IL-6 led to reduced demyelination.[51] Experimental evidence suggests that modulation of neuroinflammation is essential for effectively treating neuropathic pain, and the administration of cytokine inhibitors reduces neuropathology

and pain-related behaviors in a mouse model with brachial plexus avulsion.[52] Perineural steroid injections are commonly used to address neuropathic pain that is difficult to treat with oral medications (gabapentin, tricyclic antidepressants, and serotonin-norepinephrine reuptake inhibitors).[53] The analgesic effect of corticosteroids is based on their well-known anti-inflammatory properties, which reduce the ectopic discharge of the involved nerve and relieve mechanical pressure by reducing neuronal edema and fibrosis.[54,55] However, physicians remain concerned regarding possible steroid-related adverse effects, including hyperglycemia, axonal and myelin degeneration, skin thinning, myopathy, soft tissue atrophy, steroid flares, crystal-induced synovitis, and hypersensitivity reactions.[56,57] In general, the therapeutic effect of perineural steroid injections is relatively short-lived (<3 months) and repeated use is common in clinical practice, amplifying related concerns.[58–60] Moreover, alternative medications, such as dextrose or platelet-rich plasma, as well as hydrodissection therapy, have been explored; however, their comparative advantage remains controversial owing to different methodologies and conflicting conclusions.[56,59,61] Therefore, the development of novel therapeutic agents is of great interest.

Plant-derived bioactive compounds, often called phytochemicals (from Greek *phyto*, meaning "plant"), are active substances derived from various plants.[62] Their biological activities in plant hosts, either for plant growth or defense against competitors, pathogens, or predators, can be an excellent source for developing new promising medications.[63] Among them, vanillin (4-hydroxy-3-methoxybenzaldehyde) has recently received considerable attention for its pharmaceutical potential and bioavailability. Accumulated evidence suggests that vanillin has considerable anticancer, antidiabetic, antioxidant, antibacterial, and antidepressant properties.[64] Similar to the current study, phytochemicals and nanoparticle formulations for anti-inflammatory and antioxidative stress have been explored. In a study using zinc oxide nanoparticles synthesized with *Polygala tenuifolia* root extract, expression levels of inducible nitric oxide synthase (iNOS), COX-2, IL-1β, IL-6, and TNF-α were suppressed. In a diabetic neuropathy model,[65] silver nanoparticles formulated with *Nigella sativa* exhibited anti-inflammatory and antioxidant effects; however, additional research is crucial to ensure clinical translation.[66] The PVO nanoparticles examined in the current study are an innovative agent that can simultaneously function as a therapeutic agent and an ultrasonographic contrast agent, as they were designed to be triggered by H_2O_2 to generate CO_2 bubbles and release vanillin. To the best of our knowledge, this is the first study to assess the diagnostic value of H_2O_2-responsive nanoparticles as ultrasonographic contrast agents and their potential as therapeutic agents in a rat model of neuritis.

Herein, we observed that PVO nanoparticles could suppress the expression of TNF-α, IL-6, and COX-2 and reduce inflammatory cell infiltration, thereby exerting highly potent therapeutic activities against nerve damage. Vanillin downregulates pro-inflammatory cytokine expression by regulating nuclear factor-κB signaling, and its neuroprotective effects mediated via antioxidative (decreases in COX and nitric oxide synthase) and anti-inflammatory activities have been documented in potassium bromate-induced neurotoxicity models.[67] Several studies have explored the potential of various anti-inflammatory substances, including endogenous metabolites, phytochemicals, or experimental drugs. Moreover, regulating neuroinflammation and inflammatory cytokines, such as TNF-α, IL-1β, and IL-6, is crucial for nerve recovery and neuroprotection in peripheral nerve injury or neuropathic pain models.[68–70] This finding is consistent with that observed in previous studies. In addition, owing to its lipophilicity, vanillin may be stored and released in perineural fat, which is particularly abundant around the spinal nerve roots or nerve plexuses, to exert sustained effects.[71] In previous muscle injury model studies, PVO nanoparticles were shown to exhibit therapeutic activity by inhibiting the expression of inflammatory cytokines such as TNF-α, IL-1β, IL-6, and iNOS and also regulating apoptosis-related proteins. PVO, which specifically scavenges H_2O_2, generates CO_2, and releases vanillin at the pathological site, is an attractive nanoparticle for lesion-specific echogenic and therapeutic agents, as demonstrated in the current study.

Although this is the first study documenting the potential of PVO nanoparticles as ultrasonographic contrast and therapeutic agents in a rat model of sciatic neuritis, it is crucial to undertake further studies regarding optimal doses, concentrations, and volumes considering contrast and therapeutic effects, to comprehensively clarify the translational potential of this agent. Importantly, large animal studies using other clinically relevant models, such as subacute and chronic phase injury models, or evaluating more clinically relevant outcomes related to nerve injuries, such as pain (allodynia or hyperalgesia)-related behavior or motor function, are warranted prior to clinical translation.

Conclusions

The present study is the first to assess the diagnostic value of H_2O_2-responsive nanoparticles as ultrasonographic contrast agents and their potential as therapeutic agents in a rat neuritis model. PVO nanoparticles enhanced ultrasonographic contrast and exerted significant anti-inflammatory effects. Based on these findings, H_2O_2-responsive echogenic and anti-inflammatory PVO nanoparticles are promising next-generation agents that can facilitate the simultaneous diagnosis and treatment of nerve lesions.

Data Sharing Statement

The datasets used and/or analyzed during the current study are available from the corresponding author on reasonable request.

Ethics Approval

All animal experimental procedures were approved by the Institutional Animal Care and Use Committee (IACUC) of Jeonbuk National University Hospital (JBUH-IACUC-2021-34-1) and were performed following the regulations. Laboratory animal welfare was observed in accordance with the IACUC standard operating guidelines jointly published by Korea's Animal and Plant Quarantine Agency and the Ministry of Food and Drug Safety.

Acknowledgments

The authors thank all members of the Department of Physical Medicine Rehabilitation, Jeonbuk National University Hospital and Department of Bionanotechnology and Bioconvergence Engineering, Jeonbuk National University.

Funding

This research was supported by the National Research Foundation of Korea (NRF), a grant funded by the Korean government (MSIT) (No. 2022R1C1C1005770 and 2019R1I1A3A01061885) and by Bio&Medical Technology Development Program of the National Research Foundation (NRF) (No. RS-2023-00236157), and by grants from the Biomedical Research Institute of Jeonbuk National University Hospital, Jeonju, Korea.

Disclosure

The authors report no conflicts of interest in this work.

References

1. Keijzer F. Moving and sensing without input and output: early nervous systems and the origins of the animal sensorimotor organization. *Biol Philos*. 2015;30(3):311–331. doi:10.1007/s10539-015-9483-1
2. Sullivan R, Dailey T, Duncan K, Abel N, Borlongan CV. Peripheral nerve injury: stem cell therapy and peripheral nerve transfer. *Int J Mol Sci*. 2016;17(12):2101. doi:10.3390/ijms17122101
3. Kumar A, Kaur H, Singh A. Neuropathic pain models caused by damage to central or peripheral nervous system. *Pharmacol Rep*. 2018;70 (2):206–216. doi:10.1016/j.pharep.2017.09.009
4. Yoshii Y, Nishiura Y, Terui N, Hara Y, Ochiai N. The effects of repetitive compression on nerve conduction and blood flow in the rabbit sciatic nerve. *J Hand Surg Eur*. 2010;35(4):269–278. doi:10.1177/1753193408090107
5. Mackinnon SE. Pathophysiology of nerve compression. *Hand Clin*. 2002;18(2):231–241. doi:10.1016/S0749-0712(01)00012-9
6. Schmid AB, Coppieters MW, Ruitenberg MJ, McLachlan EM. Local and remote immune-mediated inflammation after mild peripheral nerve compression in rats. *J Neuropathol Exp Neurol*. 2013;72(7):662–680. doi:10.1097/NEN.0b013e318298de5b
7. Rothman SM, Nicholson KJ, Winkelstein BA. Time-dependent mechanics and measures of glial activation and behavioral sensitivity in a rodent model of radiculopathy. *J Neurotrauma*. 2010;27(5):803–814. doi:10.1089/neu.2009.1045
8. Moalem G, Tracey DJ. Immune and inflammatory mechanisms in neuropathic pain. *Brain Res Rev*. 2006;51(2):240–264. doi:10.1016/j.brainresrev.2005.11.004
9. Shamji MF, Allen KD, So S, et al. Gait abnormalities and inflammatory cytokines in an autologous nucleus pulposus model of radiculopathy. *Spine*. 2009;34(7):648–654. doi:10.1097/BRS.0b013e318197f013
10. Groszmann YS, Benacerraf BR. Complete evaluation of anatomy and morphology of the infertile patient in a single visit; the modern infertility pelvic ultrasound examination. *Fertil Steril*. 2016;105(6):1381–1393. doi:10.1016/j.fertnstert.2016.03.026
11. Ricci V, Ricci C, Cocco G, et al. Histopathology and high-resolution ultrasound imaging for peripheral nerve (injuries). *J Neurol*. 2022;269 (7):3663–3675. doi:10.1007/s00415-022-10988-1
12. Gallardo E, Noto Y-I, Simon NG. Ultrasound in the diagnosis of peripheral neuropathy: structure meets function in the neuromuscular clinic. *J Neurol Neurosurg Psychiatry*. 2015;86(10):1066–1074. doi:10.1136/jnnp-2014-309599

13. Cartwright MS, Walker FO. Neuromuscular ultrasound in common entrapment neuropathies. *Muscle Nerve*. 2013;48(5):696–704. doi:10.1002/mus.23900
14. Han X, Xu K, Taratula O, Farsad K. Applications of nanoparticles in biomedical imaging. *Nanoscale*. 2019;11(3):799–819. doi:10.1039/C8NR07769J
15. Hidayati HB, Subadi I, Fidiana F, Puspamaniar VA. Current diagnosis and management of carpal tunnel syndrome: a review. *Anaesth Pain Intensive Care*. 2022;26(3):394–404. doi:10.35975/apic.v26i3.1902
16. Schmid AB, Fundaun J, Tampin B. Entrapment neuropathies: a contemporary approach to pathophysiology, clinical assessment, and management. *PAIN Rep*. 2020;5(4):e829. doi:10.1097/PR9.0000000000000829
17. Yasir M, Goyal A, Sonthalia S. Corticosteroid Adverse Effects. 2018.
18. Norbury JW, Nazarian LN. Ultrasound-guided treatment of peripheral entrapment mononeuropathies. *Muscle Nerve*. 2019;60(3):222–231. doi:10.1002/mus.26517
19. López-Cebral R, Silva-Correia J, Reis RL, Silva TH, Oliveira JM. Peripheral nerve injury: current challenges, conventional treatment approaches, and new trends in biomaterials-based regenerative strategies. *ACS Biomater Sci Eng*. 2017;3(12):3098–3122. doi:10.1021/acsbiomaterials.7b00655
20. Kwon J, Kim J, Park S, Khang G, Kang PM, Lee D. Inflammation-responsive antioxidant nanoparticles based on a polymeric prodrug of vanillin. *Biomacromolecules*. 2013;14(5):1618–1626. doi:10.1021/bm400256h
21. Bezerra DP, Soares AKN, de Sousa DP. Overview of the role of vanillin on redox status and cancer development. *Oxid Med Cell Longev*. 2016;2016:9734816. doi:10.1155/2016/9734816
22. Zhao D, Sun J, Sun B, et al. Intracellular antioxidant effect of vanillin, 4-methylguaiacol and 4-ethylguaiacol: three components in Chinese baijiu. *RSC Adv*. 2017;7(73):46395–46405. doi:10.1039/C7RA09302K
23. Kim GW, Song NH, Park MR, et al. Diagnosis and simultaneous treatment of musculoskeletal injury using H_2O_2-triggered echogenic antioxidant polymer nanoparticles in a rat model of contusion injury. *Nanomaterials*. 2021;11(10):2571. doi:10.3390/nano11102571
24. Kim GW, Kang C, Oh YB, Ko MH, Seo JH, Lee D. Ultrasonographic imaging and anti-inflammatory therapy of muscle and tendon injuries using polymer nanoparticles. *Theranostics*. 2017;7(9):2463–2476. doi:10.7150/thno.18922
25. Geuna S. The sciatic nerve injury model in pre-clinical research. *J Neurosci Methods*. 2015;243:39–46. doi:10.1016/j.jneumeth.2015.01.021
26. DeLeonibus A, Rezaei M, Fahradyan V, Silver J, Rampazzo A, Bassiri Gharb B. A meta-analysis of functional outcomes in rat sciatic nerve injury models. *Microsurgery*. 2021;41(3):286–295. doi:10.1002/micr.30713
27. Khan J, Hassun H, Zusman T, Korczeniewska O, Eliav E. Interleukin-8 levels in rat models of nerve damage and neuropathic pain. *Neurosci Lett*. 2017;657:106–112. doi:10.1016/j.neulet.2017.07.049
28. Dubový P, Klusáková I, Hradilová-Svíženská I, Joukal M. Expression of regeneration-associated proteins in primary sensory neurons and regenerating axons after nerve injury-an overview. *Anat Rec*. 2018;301(10):1618–1627. doi:10.1002/ar.23843
29. Myers RR, Campana WM, Shubayev VI. The role of neuroinflammation in neuropathic pain: mechanisms and therapeutic targets. *Drug Discov Today*. 2006;11(1–2):8–20. doi:10.1016/S1359-6446(05)03637-8
30. Tao T, Ji Y, Cheng C, et al. Tumor necrosis factor-alpha inhibits Schwann cell proliferation by up-regulating Src-suppressed protein kinase C substrate expression. *J Neurochem*. 2009;111(3):647–655. doi:10.1111/j.1471-4159.2009.06346.x
31. Nadeau S, Filali M, Zhang J, et al. Functional recovery after peripheral nerve injury is dependent on the pro-inflammatory cytokines IL-1β and TNF: implications for neuropathic pain. *J Neurosci*. 2011;31(35):12533–12542. doi:10.1523/JNEUROSCI.2840-11.2011
32. Shubayev VI, Angert M, Dolkas J, Campana WM, Palenscar K, Myers RR. TNFα-induced MMP-9 promotes macrophage recruitment into injured peripheral nerve. *Mol Cell Neurosci*. 2006;31(3):407–415. doi:10.1016/j.mcn.2005.10.011
33. Cohen SP, Mao J. Neuropathic pain: mechanisms and their clinical implications. *BMJ*. 2014;348(feb05 6):f7656. doi:10.1136/bmj.f7656
34. Finnerup NB, Kuner R, Jensen TS. Neuropathic pain: from mechanisms to treatment. *Physiol Rev*. 2021;101(1):259–301. doi:10.1152/physrev.00045.2019
35. Nazemi S, Manaheji H, Noorbakhsh SM, et al. Inhibition of microglial activity alters spinal wide dynamic range neuron discharge and reduces microglial Toll-like receptor 4 expression in neuropathic rats. *Clin Exp Pharmacol Physiol*. 2015;42(7):772–779. doi:10.1111/1440-1681.12414
36. Dubový P, Jančálek R, Kubek T. Role of inflammation and cytokines in peripheral nerve regeneration. *Int Rev Neurobiol*. 2013;108:173–206.
37. Gasparotti R, Padua L, Briani C, Lauria G. New technologies for the assessment of neuropathies. *Nat Rev Neurol*. 2017;13(4):203–216. doi:10.1038/nrneurol.2017.31
38. Chung T, Prasad K, Lloyd TE. Peripheral neuropathy: clinical and electrophysiological considerations. *Neuroimaging Clin N Am*. 2014;24(1):49–65. doi:10.1016/j.nic.2013.03.023
39. Madani S, Doughty C. Lower extremity entrapment neuropathies. *Best Pract Res Clin Rheumatol*. 2020;34(3):101565. doi:10.1016/j.berh.2020.101565
40. Wijntjes J, Borchert A, van Alfen N. Nerve ultrasound in traumatic and iatrogenic peripheral nerve injury. *Diagnostics*. 2020;11(1):30. doi:10.3390/diagnostics11010030
41. Holzgrefe RE, Wagner ER, Singer AD, Daly CA. Imaging of the peripheral nerve: concepts and future direction of magnetic resonance neurography and ultrasound. *J Hand Surg Am*. 2019;44(12):1066–1079. doi:10.1016/j.jhsa.2019.06.021
42. Christensen-Jeffries K, Couture O, Dayton PA, et al. Super-resolution ultrasound imaging. *Ultrasound Med Biol*. 2020;46(4):865–891. doi:10.1016/j.ultrasmedbio.2019.11.013
43. de Jong N, Emmer M, van Wamel A, Versluis M. Ultrasonic characterization of ultrasound contrast agents. *Med Biol Eng Comput*. 2009;47(8):861–873. doi:10.1007/s11517-009-0497-1
44. Frinking P, Segers T, Luan Y, Tranquart F. Three decades of ultrasound contrast agents: a review of the past, present and future improvements. *Ultrasound Med Biol*. 2020;46(4):892–908. doi:10.1016/j.ultrasmedbio.2019.12.008
45. Fischer C, Krix M, Weber M-A, et al. Contrast-enhanced ultrasound for musculoskeletal applications: a world federation for ultrasound in medicine and biology position paper. *Ultrasound Med Biol*. 2020;46(6):1279–1295. doi:10.1016/j.ultrasmedbio.2020.01.028
46. Wang S, Hossack JA, Klibanov AL. Targeting of microbubbles: contrast agents for ultrasound molecular imaging. *J Drug Target*. 2018;26(5–6):420–434. doi:10.1080/1061186X.2017.1419362
47. Eliav E, Herzberg U, Ruda MA, Bennett GJ. Neuropathic pain from an experimental neuritis of the rat sciatic nerve. *Pain*. 1999;83(2):169–182. doi:10.1016/S0304-3959(99)00102-5

48. Boon AJ, Smith J, Harper CM. Ultrasound applications in electrodiagnosis. *PM R*. 2012;4(1):37–49. doi:10.1016/j.pmrj.2011.07.004
49. Park H, Kim S, Kim S, et al. Antioxidant and anti-inflammatory activities of hydroxybenzyl alcohol releasing biodegradable polyoxalate nanoparticles. *Biomacromolecules*. 2010;11(8):2103–2108. doi:10.1021/bm100474w
50. Liefner M, Siebert H, Sachse T, Michel U, Kollias G, Brück W. The role of TNF-α during Wallerian degeneration. *J Neuroimmunol*. 2000;108(1–2):147–152. doi:10.1016/S0165-5728(00)00262-9
51. Nishimoto S, Okada K, Tanaka H, et al. Neurotropin attenuates local inflammatory response and inhibits demyelination induced by chronic constriction injury of the mouse sciatic nerve. *Biologicals*. 2016;44(4):206–211. doi:10.1016/j.biologicals.2016.03.005
52. Quintão NL, Balz D, Santos AR, Campos MM, Calixto JB. Long-lasting neuropathic pain induced by brachial plexus injury in mice: role triggered by the pro-inflammatory cytokine, tumour necrosis factor α. *Neuropharmacology*. 2006;50(5):614–620. doi:10.1016/j.neuropharm.2005.11.007
53. Cruccu G, Truini A. A review of neuropathic pain: from guidelines to clinical practice. *Pain Ther*. 2017;6(S1):35–42. doi:10.1007/s40122-017-0087-0
54. Eker HE, Cok OY, Aribogan A, Arslan G. Management of neuropathic pain with methylprednisolone at the site of nerve injury. *Pain Med*. 2012;13(3):443–451. doi:10.1111/j.1526-4637.2011.01323.x
55. Choi YK. Lumbar foraminal neuropathy: an update on non-surgical management. *Korean J Pain*. 2019;32(3):147–159. doi:10.3344/kjp.2019.32.3.147
56. Lam KHS, Wu YT, Reeves KD, Galluccio F, Allam AE, Peng PWH. Ultrasound-guided interventions for carpal tunnel syndrome: a systematic review and meta-analyses. *Diagnostics*. 2023;13(6):1138. doi:10.3390/diagnostics13061138
57. Wu YT, Ke MJ, Ho TY, Li TY, Shen YP, Chen LC. Randomized double-blinded clinical trial of 5% dextrose versus triamcinolone injection for carpal tunnel syndrome patients. *Ann Neurol*. 2018;84(4):601–610. doi:10.1002/ana.25332
58. Wu YT, Ho TY, Chou YC, et al. Six-month efficacy of perineural dextrose for carpal tunnel syndrome: a prospective, randomized, double-blind, controlled trial. *Mayo Clin Proc*. 2017;92(8):1179–1189. doi:10.1016/j.mayocp.2017.05.025
59. Chen LC, Ho TY, Shen YP, et al. Perineural dextrose and corticosteroid injections for ulnar neuropathy at the elbow: a randomized double-blind trial. *Arch Phys Med Rehabil*. 2020;101(8):1296–1303. doi:10.1016/j.apmr.2020.03.016
60. Marshall SC, Tardif G, Ashworth NL. Local corticosteroid injection for carpal tunnel syndrome. *Cochrane Database Syst Rev*. 2007;2:CD001554.
61. Shen YP, Li TY, Chou YC, et al. Comparison of perineural platelet-rich plasma and dextrose injections for moderate carpal tunnel syndrome: a prospective randomized, single-blind, head-to-head comparative trial. *J Tissue Eng Regen Med*. 2019;13(11):2009–2017. doi:10.1002/term.2950
62. Frank J, Fukagawa NK, Bilia AR, et al. Terms and nomenclature used for plant-derived components in nutrition and related research: efforts toward harmonization. *Nutr Rev*. 2020;78(6):451–458. doi:10.1093/nutrit/nuz081
63. Rahman MM, Dhar PS, Sumaia S, et al. Exploring the plant-derived bioactive substances as antidiabetic agent: an extensive review. *Biomed Pharmacother*. 2022;152:113217. doi:10.1016/j.biopha.2022.113217
64. Olatunde A, Mohammed A, Ibrahim MA, Tajuddeen N, Shuaibu MN. Vanillin: a food additive with multiple biological activities. *Eur J Med Chem Rep*. 2022;5:100055.
65. Nagajyothi PC, Cha SJ, Yang IJ, Sreekanth TV, Kim KJ, Shin HM. Antioxidant and anti-inflammatory activities of zinc oxide nanoparticles synthesized using *Polygala tenuifolia* root extract. *J Photochem Photobiol B*. 2015;146:10–17. doi:10.1016/j.jphotobiol.2015.02.008
66. Alkhalaf MI, Hussein RH, Hamza A. Green synthesis of silver nanoparticles by *Nigella sativa* extract alleviates diabetic neuropathy through anti-inflammatory and antioxidant effects. *Saudi J Biol Sci*. 2020;27(9):2410–2419. doi:10.1016/j.sjbs.2020.05.005
67. Ben Saad H, Kharrat N, Driss D, et al. Effects of vanillin on potassium bromate-induced neurotoxicity in adult mice: impact on behavior, oxidative stress, genes expression, inflammation and fatty acid composition. *Arch Physiol Biochem*. 2017;123(3):165–174. doi:10.1080/13813455.2017.1283527
68. Casadei M, Fiore E, Rubione J, et al. IMT504 blocks allodynia in rats with spared nerve injury by promoting the migration of mesenchymal stem cells and by favoring an anti-inflammatory *milieu* at the injured nerve. *Pain*. 2022;163(6):1114–1129. doi:10.1097/j.pain.0000000000002476
69. Kandhare AD, Mukherjee AA, Bodhankar SL. Neuroprotective effect of *Azadirachta indica* standardized extract in partial sciatic nerve injury in rats: evidence from anti-inflammatory, antioxidant and anti-apoptotic studies. *Excli J*. 2017;16:546–565. doi:10.17179/excli2017-161
70. Starinets A, Tyrtyshnaia A, Manzhulo I. Anti-inflammatory activity of synaptamide in the peripheral nervous system in a model of sciatic nerve injury. *Int J Mol Sci*. 2023;24(7):6273. doi:10.3390/ijms24076273
71. Beaudry F, Ross A, Lema PP, Vachon P. Pharmacokinetics of vanillin and its effects on mechanical hypersensitivity in a rat model of neuropathic pain. *Phytother Res*. 2010;24(4):525–530. doi:10.1002/ptr.2975